Thermochimica Acta 479 (2008) 37–44

Contents lists available at ScienceDirect

Thermochimica Acta

journal homepage: www.elsevier.com/locate/tca

Kinetic study by FTIR and DSC on the cationic curing of a DGEBA/γ-valerolactone mixture with ytterbium triflate as an initiator

M. Arasa [a], X. Ramis [b,*], J.M. Salla [b], A. Mantecón [a], A. Serra [a]

[a] Departament de Química Analítica i Química Orgànica, Universitat Rovira i Virgili. C/Marcel·lí Domingo s/n, 43007 Tarragona, Spain
[b] Laboratori de Termodinàmica, ETSEIB. Universitat Politècnica de Catalunya, Av. Diagonal 647, 08028 Barcelona, Spain

ARTICLE INFO

Article history:
Received 9 July 2008
Received in revised form
10 September 2008
Accepted 21 September 2008
Available online 1 October 2008

Keywords:
Epoxy resins
Ytterbium triflate
Kinetics
Cationic polymerization
Thermosets
Lactones

ABSTRACT

A mixture of diglycidylether of bisphenol A (DGEBA) and γ-valerolactone (γ-VL) was cured in the presence of ytterbium triflate as an initiator to obtain poly(esther-ether) thermosets. The kinetics of the various elemental reactions, which take place during the curing process, was studied by means of isothermal curing in the FTIR spectrometer. The kinetic parameters were calculated by means of the isoconversional procedure and the best-fit kinetic model was determined with the so-called compensation effect (isokinetic relationship). The isothermal kinetic analysis was compared with that obtained by dynamic curing in DSC.

1. Introduction

It is well known that internal stress usually occurs during the curing of epoxide resins and causes various defects, e.g., microcracks, microvoids, and delamination [1,2], which reduce their durability and make worse their properties. Therefore, one of the main subjects in the field of epoxide resin technology is to prevent or reduce the internal stress generated in the thermoset. During the 1970s, Bailey et al. [3–6] described in various papers that some spiroorthoesters (SOEs) polymerize with expansion in volume or with very low shrinkage. Therefore, they applied the term *expanding monomers* to these compounds. Among the expanding monomers, they also considered spiroorthocarbonates (SOCs) and bicycloorthoesters (BOEs), but SOEs were the most promising monomers of this type. The classical synthetic procedure applied in their synthesis consists of reacting epoxides and lactones in the presence of a Lewis acid [7]. The corresponding SOEs can polymerize in cationic medium to yield poly(ether-ester)s via a double-tandem ring opening process.

Conventionally, BF_3 complexes are used as Lewis acid due to their latent character [8–10], but as an alternative we used lanthanide triflates in the polymerization of these compounds. Lanthanide triflates are stable in water, act as Lewis acid initiators, can be recovered [11,12], and are capable of cross-linking pure glycidylic and cycloaliphatic epoxy resins or their mixtures with lactones [13–15]. In a previous study [16], we polymerized diglycidylether of bisphenol A (DGEBA) with γ-butyrolactone (γ-BL) using ytterbium triflate as an initiator. Although the global shrinkage was not reduced, by means of thermomechanical analysis (TMA) we proved that the addition of γ-BL to the DGEBA led to materials with lower contraction after gelation and therefore with lower internal stresses. The explanation to this behavior is based in the complex reaction mechanism. During the curing process four chemical processes coexist: (a) formation of SOE by reaction of DGEBA with γ-lactone, (b) homopolymerization of epoxy groups, (c) homopolymerization of SOE, and (d) copolymerization of SOE with epoxy groups (Scheme 1). Because SOEs homopolymerize or copolymerize with some expansion in the final stages of the curing, the contraction after gelation is reduced. Thus, the main contraction is produced when the material is a viscous liquid and in this way the internal stresses are reduced. The knowledge of the kinetics of the elemental reactions that takes place during curing could allow estimating the times necessary to complete these processes. In this way it could be possible to relate these times with the shrinkage that occurs and also with the stresses generated in the thermoset on curing.

* Corresponding author. Tel.: +34 934016592; fax: +34 934017389.
E-mail address: ramis@mmt.upc.edu (X. Ramis).

0040-6031/$ – see front matter © 2008 Elsevier B.V. All rights reserved.
doi:10.1016/j.tca.2008.09.020

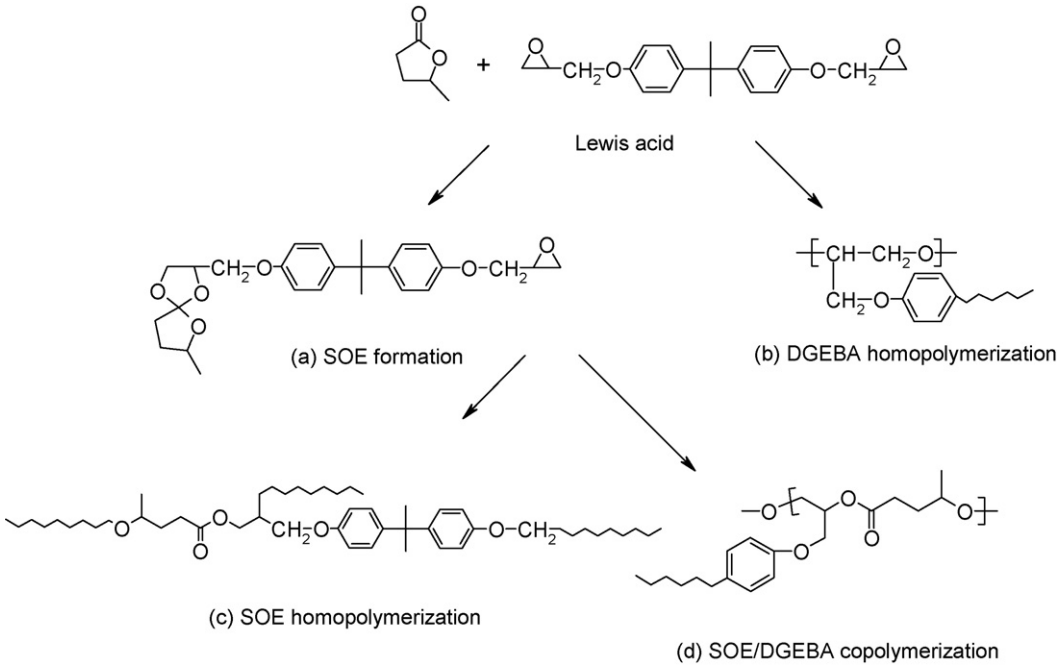

Scheme 1. Individual reactions expected in the curing for DGEBA with γ-VL.

FTIR-ATR can be applied to investigate the evolution of the different chemical reactions. By this technique detailed information can be obtained through the evolution of the absorption bands of the carbonyl and epoxy groups vs. time at several temperatures. From these conversion plots, by integral isoconversional analysis, activation energy and a second parameter (which is related to the pre-exponential factor and to the integral conversion function, which depends on the degree of conversion and represents the kinetic model that governs the process) can be calculated.

An alternative procedure to obtain kinetic parameters is by means of dynamic DSC experiments, which allows simulating the behavior during the isothermal curing [17]. However, DSC gives only information of the overall process but not on the elemental reactions that occur during curing and should be complemented with other techniques, such as FTIR.

The present study focuses on the kinetic analysis of the curing of mixtures of DGEBA with γ-VL using ytterbium triflate as an initiator. We studied the kinetics of the elemental reactions that are part of the curing by FTIR spectroscopy and the overall curing kinetics by DSC. Eventually, we propose a method that uses the isoconversional isothermal parameters determined by FTIR and the compensation effect [18–20] to calculate the complete kinetic triplet. The results were compared with those obtained by nonisothermal procedures.

2. Experimental

2.1. Materials

Diglycidylether of bisphenol A (DGEBA) EPIKOTE RESIN 827 (epoxy equiv. = 182.1 g/equiv.) (Shell Chemicals), γ-valerolactone (γ-VL) and ytterbium(III) trifluoromethanesulfonate (Aldrich) were used as received.

2.2. Preparation of the curing mixtures

The mixture was prepared by dissolving 1 phr (one part per hundred parts of mixture, w/w) of ytterbium triflate in 0.01 mol of γ-VL and adding 0.02 mol of DGEBA. The sample was kept at −18 °C before use.

2.3. FTIR spectroscopy

The isothermal curing process, between 120 and 160 °C, was monitored with a FTIR 680 Plus from Jasco with 4 cm^{-1} of resolution in the absorbance mode. An attenuated total reflection accessory with thermal control and a diamond crystal (a Golden Gate heated single-reflection diamond ATR from Specac-Teknokroma) was used to determine FTIR spectra. The disappearance of the 910 and 1775 cm^{-1} absorbance peak (epoxy bending and carbonyl C=O stretching of cyclic ester) was used to monitor the epoxy and γ-VL conversion, respectively. The formation of the 1737 cm^{-1} absorbance peak (carbonyl C=O stretching of aliphatic linear ester), which does not exist in the sample before curing, indicates that ring-opening polymerization of SOE has occurred. Thus, this let us to evaluate the linear ester formation. The peak at 1605 cm^{-1} (phenyl group) was chosen as an internal standard. Conversions of the different reactive groups, epoxy, lactone and linear ester, were determined by the Lambert-Beer law from the normalized changes of absorbance at 910, 1775, and 1737 cm^{-1} [10,16,21]:

$$\alpha_{\text{epoxy}} = 1 - \left(\frac{\bar{A}^t_{910}}{\bar{A}^0_{910}}\right), \qquad \alpha_{\gamma\text{-VL}} = 1 - \left(\frac{\bar{A}^t_{1775}}{\bar{A}^0_{1775}}\right),$$
$$\alpha_{\text{SOE}} = \left(\frac{\bar{A}^t_{1737}}{\bar{A}^\infty_{1737}}\right) \tag{1}$$

where $\bar{A}^0$, $\bar{A}^t$ and $\bar{A}^\infty$ are the normalized absorbance of the reactive groups before curing, after reaction time t, and after complete curing, respectively ($\bar{A}^0_{910} = A^0_{910}/A^0_{1605}$; $\bar{A}^0_{1775} = A^0_{1775}/A^0_{1605}$; $\bar{A}^t_{910} = A^t_{910}/A^t_{1605}$; $\bar{A}^t_{1775} = A^t_{1775}/A^t_{1605}$; $\bar{A}^t_{1737} = A^t_{1737}/A^t_{1605}$; $\bar{A}^\infty_{1737} = A^\infty_{1737}/A^\infty_{1605}$).

2.4. Differential scanning calorimetry

Calorimetric analyses were carried out on a Mettler DSC-821e thermal analyzer using N_2 as a purge gas in covered aluminium pans. The weight of the samples was approximately 5 mg. Non-isothermal curing was carried out at rates of 2, 5, 10 and 15 K/min and the degree of conversion was calculated as:

$$\alpha_{DSC} = \frac{\Delta H_T}{\Delta H_{dyn}} \tag{2}$$

where ΔH_T is the heat released up to a temperature T, obtained by integrating the calorimetric signal up to that temperature, and ΔH_{dyn} is the total reaction heat associated with complete conversion of all reactive groups determined for each heating rate.

3. Kinetic analysis

If we accept that the dependence of the rate constant on the temperature follows the Arrhenius equation, the kinetics of the reaction is usually described by the following rate equation:

$$\frac{d\alpha}{dt} = Af(\alpha)\exp\left(-\frac{E}{RT}\right) \tag{3}$$

where t is time, A is the pre-exponential factor, E is the activation energy, T is the absolute temperature, R is the gas constant, and $f(\alpha)$ is the kinetic model.

In general, the kinetic analysis was carried out using an isoconversional method. The basic assumption of these methods is that the reaction rate at constant conversion is only function of the temperature [22,23].

3.1. Isothermal methods

By integrating the rate equation [Eq. (3)] in isothermal conditions we obtain:

$$\ln t = \ln\left[\frac{g(\alpha)}{A}\right] + \frac{E}{RT} \tag{4}$$

where $g(\alpha)$ is the integral conversion function, defined as:

$$g(\alpha) = \int_0^\alpha \frac{d\alpha}{f(\alpha)} \tag{5}$$

According to Eq. (4) the activation energy and the constant $\ln[g(\alpha)/A]$ can be obtained, respectively, from the slope and the intercept of the linear relationship $\ln t$ against $1/T$ for α = constant.

3.2. Nonisothermal methods

By integrating Eq. (3) in nonisothermal conditions and reordering it, the so-called temperature integral can be expressed as:

$$g(\alpha) = \int_0^\alpha \frac{d\alpha}{f(\alpha)} = \frac{A}{\beta}\int_0^T e^{-(E/RT)}\,dT \tag{6}$$

where β is the heating rate.

By using the Coats–Redfern [24] approximation to solve Eq. (6), and considering that $2RT/E$ is much lower than 1, the term $(1-2RT/E)$ can be neglected and the solution of the temperature integral may be expressed as [25]:

$$\ln\frac{g(\alpha)}{T^2} = \ln\left[\frac{AR}{\beta E}\right] - \frac{E}{RT} \tag{7}$$

For a given kinetic model, linear representation of $\ln[g(\alpha)/T^2]$ against $1/T$ makes it possible to determine E and A from the slope and the ordinate at the origin. In this work, we selected the kinetic model that had the best linear correlation in the Coats–Redfern equation and that had an E value similar to that obtained isoconversionally (considered to be effective E value).

By reordering Eq. (7) we can write the Kissinger–Akahira–Sunose (KAS) equation [26,27]:

$$\ln\frac{\beta}{T^2} = \ln\left[\frac{AR}{g(\alpha)E}\right] - \frac{E}{RT} \tag{8}$$

For each conversion degree, the linear plot of $\ln[\beta/T^2]$ against $1/T$ enables E and the kinetic parameter $\ln[AR/g(\alpha)E]$ to be determined from the slope and the intercept. If the model, $g(\alpha)$, is known, the corresponding pre-exponential factor can be calculated from each conversion. This isoconversional procedure is similar to Flynn–Wall–Ozawa's method [28–30].

The constant $\ln[AR/g(\alpha)E]$ is directly related by R/E to the constant $\ln[g(\alpha)/A]$ of the isothermal adjustment [Eq. (4)]. Thus, taking the dynamic data $\ln[AR/g(\alpha)E]$ and E, and applying Eq. (8), we can determine the isoconversional lines [Eq. (4)] and simulate isothermal curing [31,17].

3.3. Compensation effect (isokinetic relationship)

For complex processes (parallel reactions, successive reactions, physical changes, etc.) it is characteristic for the activation energy and the pre-exponential factor to depend on the degree of conversion. This generally reflects the existence of a compensation effect through the following equation [18,20,32,33]:

$$\ln A_\alpha = aE_\alpha + b = \frac{E_\alpha}{RT} + \ln\left[\frac{(d\alpha/dt)_\alpha}{f(\alpha)}\right] \tag{9}$$

where a and b are constants, and subscript α refers to degree of conversion, that is a factor producing a change in Arrhenius parameters in this study.

The slope $a = 1/RT_{iso}$ is related to isokinetic temperature T_{iso} and the intercept $b = \ln k_{iso}$ is related to the isokinetic rate constant. Eq. (9) represents an isokinetic relationship (IKR), which can be observed as a common point of intersection of the Arrhenius lines (i.e., $\ln k$ vs. $1/T$) of a series of reactions (in this work the different degree of conversion). This intersection is characterized by a k_{iso} and a T_{iso}. By reordering and applying logarithms to Eq. (3), the Eq. (9) can be deduced.

The appearance of the IKR shows that only one mechanism is present and that all reactions have analogous reaction profiles, whereas the existence of parameters that do not agree with the IKR implies that there are multiple reaction mechanisms [34,35]. According to certain authors, we selected the kinetic model whose IKR had the best linear correlation and in which the associated T_{iso} value was near the experimental temperature range [36].

The aim of this study was to determine the complete kinetic triplet [E, A, $g(\alpha)$] in complex systems with $E = E(\alpha)$, by using isoconversional kinetic parameters, the slope and intercept of Eqs. (4) and (8), and the isokinetic relation, Eq. (9). Eq. (9) was applied to the isothermal and nonisothermal isoconversional data when the conversion changes for different kinetic models. A similar procedure was proposed by Vyazovkin to obtain the kinetic triplet [36].

4. Results and discussion

The curing process of DGEBA with γ-lactones takes place by the complex reaction mechanism depicted in Scheme 1.

Fig. 1 shows the FTIR spectra of the mixture DGEBA/γ-VL 2:1 (mol/mol) with 1 phr of $Yb(OTf)_3$ before and after curing and at

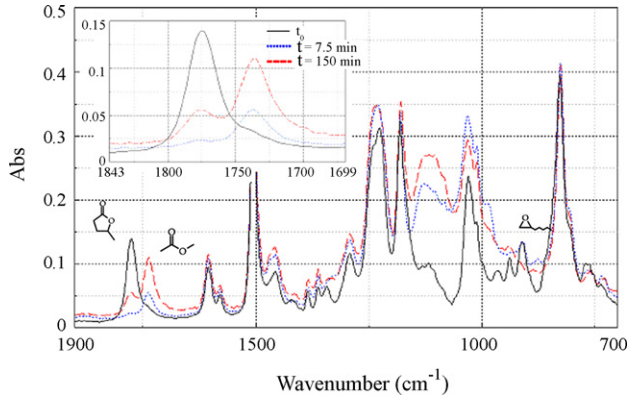

Fig. 1. FTIR-ATR spectra of a mixture of DGEBA/γ-VL in a molar ratio of 2:1 with 1 phr of $Yb(OTf)_3$ registered at different curing times at 160 °C.

intermediate time of 7.5 min, performed at 160 °C. During the curing process there are changes mainly in three typical bands:

1. The carbonyl stretching band of γ-VL at 1775 cm^{-1}, which decreases because γ-VL reacts with the epoxide groups to form SOEs. In the final stages of the curing this absorption slightly increases again, due to the reversibility of the formation of SOE groups as previously reported [15].
2. The peak at 1737 cm^{-1}, attributable to the linear aliphatic ester, increases steadily and confirms that the ring-opening polymerization of SOE occurs by homo- or co-polymerization with epoxide. In general, homopolymerization is less favourable and it is only important at the end of curing when there are few epoxide groups [16].
3. The band at 910 cm^{-1}, associated with the oxirane ring, disappears indicating that the epoxide completely polymerizes. Taking into account the stoichiometry of the formulation (4 equiv. epoxy per 1 equiv. of lactone), the epoxy group, in addition to the reaction with γ-VL, can also homopolymerize and copolymerize with SOE.

After isothermal curing in the FTIR/ATR, the complete disappearance of the epoxy groups and the absence of residual enthalpy in a DSC scan allowed us to conclude that the material was completely cured. This result is coherent with the fact that all curing temperatures are higher than the glass transition temperature of the material completely cured ($T_g^\infty = 93$ °C, determined at 10 °C/min after nonisothermal curing between 0 and 250 °C) so that vitrification during curing is not possible.

Due to the partial overlapping of carbonylic lactone and ester absorbances (between 1825 and 1670 cm^{-1}) we deconvoluted the spectroscopic signals in this zone to quantify the absorptions associated with each carbonyl group [37]. Fig. 2 shows an example of this deconvolution.

Fig. 3 shows the evolution of the conversions (corresponding to lactone and epoxide disappearance and to SOE appearance) vs. time. At first sight, it seems that the lactone reacts at short time more than epoxide, but we should consider that the proportion of epoxy groups to lactone is 4:1 and therefore that observation is not true. After 900 s at 140 °C, the lactone, which was run out, appears again. This appearance occurs when the epoxide has completely reacted and is due to the reversion of the SOEs. This process also leads to the formation of epoxide groups which immediately homopolymerize. After 1000 s of curing, SOEs disappear very quickly.

In Fig. 4 the conversion of γ-VL ($\alpha_{\gamma\text{-VL}}$) is plotted against α_{epoxy} and α_{SOE}. The SOE conversion was evaluated by the formation of linear ester band, which appears on the SOE opening. Before looking at this figure, we should take into account that: (a) the molar ratio DGEBA/γ-VL is 2:1, (b) DGEBA has 2 equiv. of epoxide per mol, (c) each mol of γ-VL reacts with 1 equiv. of epoxide to produce one mole of SOE, and (d) the homopolymerization of five-membered lactones is a thermodynamically unfavourable process. With these considerations, for $\alpha_{\gamma\text{-VL}} \sim 0.4$ we can expect that the epoxy consumption (α_{epoxy}) should be 0.1, similar as it is found experimentally (0.125). Thus, we can conclude that until $\alpha_{\gamma\text{-VL}} \sim 0.4$ the main reaction is the SOE formation.

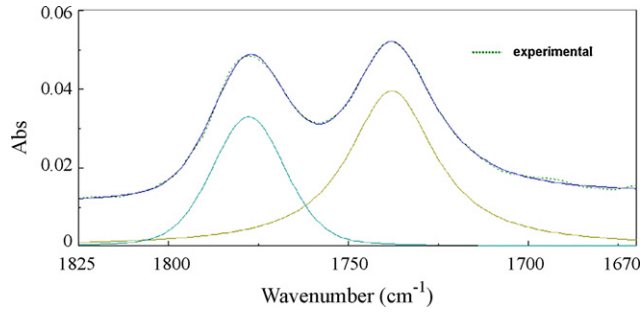

Fig. 2. Cyclic and linear carbonyl ester absorption region of the FTIR-ATR spectra of the mixture DGEBA/γ-VL (2:1 molar) catalyzed by 1 phr of $Yb(OTf)_3$ cured a 160 °C. Dotted green line corresponds to the experimental values and the other lines are obtained by deconvolution.

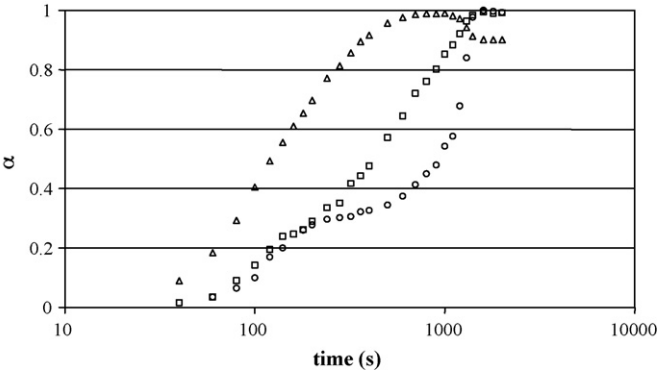

Fig. 3. Plot of the experimental degrees of (□) epoxy, (Δ) γ-VL and (○) SOE conversion vs. curing time for the sample cured at 140 °C.

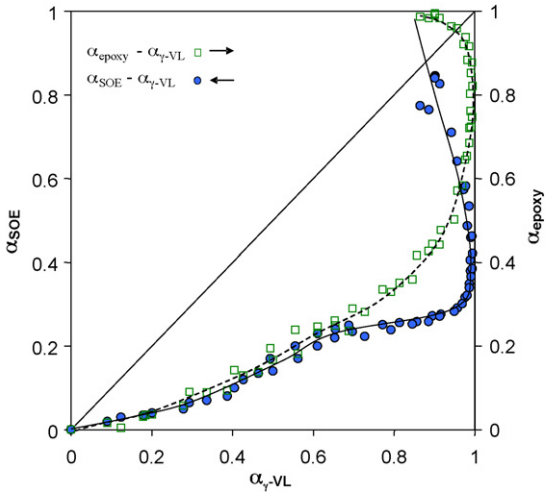

Fig. 4. Plot of the experimental $\alpha_{\gamma\text{-VL}}$ vs. α_{SOE} and $\alpha_{\gamma\text{-VL}}$ vs. α_{epoxy} obtained at several temperatures.

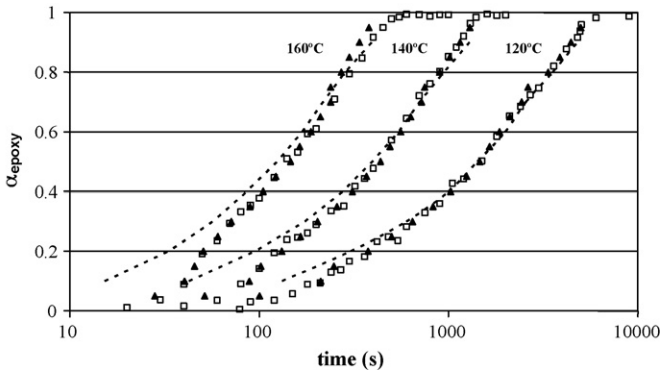

Fig. 5. Plot of the experimental and simulated degrees of epoxy conversion vs. curing times for samples cured at different temperatures: (□) experimental isothermal curves and (▲) isoconversional isothermal data obtained by Eq. (4) and (---) isoconversional nonisothermal data obtained by Eq. (8).

In Fig. 4 we can also see that when $\alpha_{\gamma\text{-VL}} \sim 0.4$, the SOE conversion is 0.1. If the copolymerisation of SOE and epoxide occurs, an additional consumption of $\alpha_{epoxy} = 0.025$ should be expected. Because of the total consumption of epoxide (α_{epoxy}) is 0.125 at $\alpha_{\gamma\text{-VL}} = 0.4$, we can confirm that SOE preferentially copolymerizes with epoxide in the first stages of curing. After $\alpha_{\gamma\text{-VL}} = 0.4$ the homopolymerization of epoxides can occur. The SOE polymerization takes mainly place when practically there is no lactone in the mixture $\alpha_{\gamma\text{-VL}} \sim 1$. That is because epoxy groups firstly prefer to react with lactones. When epoxy groups have almost disappeared, the band of γ-VL appears again. It seems that the remaining SOE groups prefer to revert to γ-VL and epoxy groups rather than homopolymerize, in contrast with what was observed in the curing of DGEBA/γ-BL mixtures [16]. In γ-BL mixtures, after the exhaustion of all epoxy groups, SOEs began to homopolymerize. The reversion of SOE in the present case can be attributed to the presence of the methyl group in the lactone [15].

Figs. 5–7 show the plots of the degree of conversion of epoxide, lactone and SOE, respectively, against time, at several curing temperatures. These experimental curves were used to determine the isoconversional kinetics of each reactive process. By applying Eq. (4) at different crosslinking degrees we obtained the kinetic parameters collected in Table 1 for each reactive group. The precision of the applied isoconversional analyses is confirmed by the good regression of the isoconversional lines. As we can see, in general, both the activation energy and the pre-exponential factor increase along the curing process in all cases. The reactive processes associated to the epoxide and SOE groups present similar activation energies,

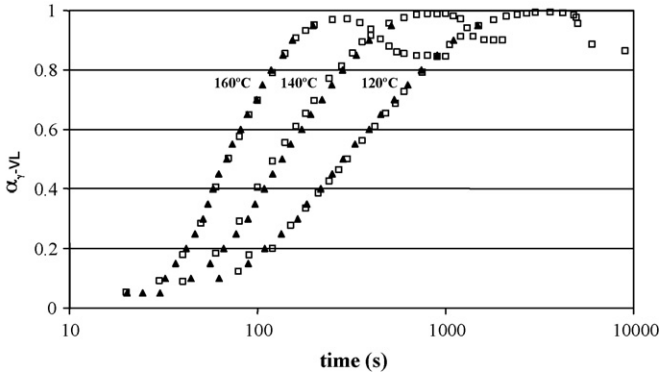

Fig. 6. Plot of the experimental and simulated degrees of γ-VL conversion vs. curing time for samples cured at different temperatures: (□) experimental isothermal curves and (▲) isoconversional isothermal data obtained by Eq. (4).

Table 1
Kinetic parameters of the curing obtained by FTIR for DGEGA/γ-VL reactive system catalyzed by ytterbium triflate.

α	Epoxy (910 cm^{-1})					γ-Valerolactone (1775 cm^{-1})					SOE (1737 cm^{-1})				
	E (kJ/mol)	ln[$g(\alpha)$/A] (s)	ln A (s^{-1})	$k_{140\,°C} \times 10^2$ (s^{-1})	r	E (kJ/mol)	ln[$g(\alpha)$/A] (s)	ln A (s^{-1})	$k_{140\,°C} \times 10^2$ (s^{-1})	r	E (kJ/mol)	ln[$g(\alpha)$/A] (s)	ln A (s^{-1})	$k_{140\,°C} \times 10^2$ (s^{-1})	r
0.1	58.6	−12.59	10.34	0.12	0.9999	23.4	−3.02	0.77	0.24	0.9989	57.0	−12.05	9.80	0.11	0.9999
0.2	70.9	−15.78	14.28	0.17	0.9991	34.1	−5.74	4.24	0.34	0.9997	68.0	−14.82	13.32	0.15	0.9998
0.3	77.9	−17.39	16.36	0.18	0.9997	40.9	−7.42	6.39	0.40	0.9994	59.0	−11.56	10.52	0.13	0.9998
0.4	80.6	−17.74	17.10	0.16	1.0000	46.6	−8.89	8.22	0.47	0.9991	72.6	−14.66	13.99	0.08	1.0000
0.5	81.4	−17.64	17.27	0.16	0.9999	50.3	−9.76	9.39	0.51	0.9989	79.2	−16.22	15.85	0.07	1.0000
0.6	81.1	−17.31	17.22	0.16	0.9997	55.7	−11.08	10.99	0.53	0.9990	86.9	−18.28	18.19	0.08	0.9999
0.7	82.1	−17.34	17.53	0.17	0.9991	59.7	−11.99	12.18	0.55	0.9997	88.2	−18.54	18.73	0.09	0.9994
0.8	89.0	−19.13	19.60	0.18	0.9998	65.1	−13.31	13.79	0.57	0.9990	86.6	−18.02	18.50	0.12	0.9992
0.9	91.0	−19.46	20.29	0.20	1.0000	69.7	−14.34	15.18	0.59	0.9992	85.6	−17.67	18.51	0.16	0.9988

α refers to α_{epoxy}, $\alpha_{\gamma\text{-VL}}$ and α_{SOE} depending on the absorbance peak used. The intercept and the slope of the isoconversional relationship $\ln t = \ln[g(\alpha)/A] + ER/T$ of the experimental data let us to obtain $\ln[g(\alpha)/A]$ and E. $\ln A$ was calculated using kinetic model F1 and $\ln[g(\alpha)/A]$.

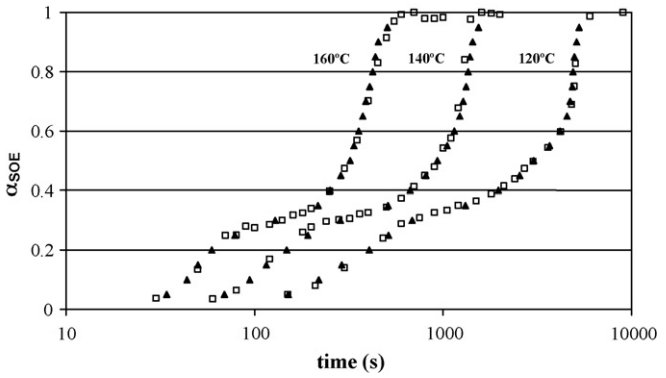

Fig. 7. Plot of the experimental and simulated degrees of SOE conversion vs. curing time for samples cured at different temperatures: (□) experimental isothermal curves and (▲) isoconversional isothermal data obtained by Eq. (4).

whereas in the process in which lactone takes part the E value is substantially lower and it reacts at shorter times. In spite of the significance of the changes observed in the kinetic parameters, it is difficult to precisely know their meaning, because of the compensation effect between activation energy and pre-exponential factor. Thus, for a better comparison of the results it is necessary to know the rate constant, k, because it includes the effect of both parameters.

To determine k from the isoconversional parameters E and $\ln[g(\alpha)/A]$, first of all it is necessary to know the kinetic model that describes the reactive process, and then to evaluate the pre-exponential factor to finally calculate k, through the Arrhenius equation.

To determine the best-fit kinetic model $g(\alpha)$, which describes the reactive process during curing, we used the isoconversional parameters (Table 1) and the isokinetic relationships. From the parameter $\ln[g(\alpha)/A]$ we obtained the pre-exponential factor for the different kinetic models used (Table 2). Then, we evaluated the isokinetic relationship, Eq. (9), for all the models and processes studied. The results are collected in Table 3 (the different T_{iso} were determined from the slopes of the IKRs). Although some models have good IKR, we considered that, in general, for all processes F1 model is the most suitable because of its good regression and its T_{iso} lying on the experimental temperature range [36] (the T_{iso} obtained for epoxy groups is 124 °C, for γ-VL 115 °C and for SOE groups 147 °C). Although, there are other models with good regression, that could also be used to describe the curing, a model of $n = 1$ order (F1), of deaccelerative type, is consistent to describe the cationic curing of epoxy systems, in which the reaction rate decreases when the concentration of reactive species decreases. Fig. 8 shows the IKR plots of the reactive species for the F1 model. We can see that epoxy and SOE groups present similar IKR, whereas γ-VL has a slightly different value. These differences can be related with the different reactivity observed in Fig. 3.

In isothermal curings, using the conventional kinetic methods, if the kinetic mechanism is unknown, it is not possible to determine the kinetic triplet. With the applied methodology we can determine the kinetic triplet by using the isoconversional parameters E and $\ln[g(\alpha)/A]$, taking into account that both parameters are related by means of the isokinetic relationships.

In Table 1 we can see the pre-exponential factors and the k at 140 °C determined using the F1 model. We can observe as $k_{\gamma\text{-VL}}$ values progressively increase due to the easiness in which the lactone reacts with the high quantity of epoxy groups that are in the mixture and to the formation of more active initiating species. In epoxy data, the values of k are in general constant but after conversion $\alpha = 0.6$, when there is not remaining lactone, these values slightly increase. This agrees with k_{SOE} values that increase, which seems to indicate that the copolymerization reaction becomes more important because the rest of the epoxy groups are available to react with SOE groups.

Table 2
Algebraic expressions for $f(\alpha)$ and $g(\alpha)$ for the kinetic model used.

Model	$f(\alpha)$	$g(\alpha)$
A3/2	$(3/2)(1-\alpha)[-\ln(1-\alpha)]^{1/3}$	$[-\ln(1-\alpha)]^{2/3}$
A2	$2(1-\alpha)[-\ln(1-\alpha)]^{1/2}$	$[-\ln(1-\alpha)]^{1/2}$
A3	$3(1-\alpha)[-\ln(1-\alpha)]^{2/3}$	$[-\ln(1-\alpha)]^{1/3}$
A4	$4(1-\alpha)[-\ln(1-\alpha)]^{3/4}$	$[-\ln(1-\alpha)]^{1/4}$
R2	$2(1-\alpha)^{1/2}$	$1-(1-\alpha)^{1/2}$
R3	$3(1-\alpha)^{2/3}$	$1-(1-\alpha)^{1/3}$
D1	$1/2(1-\alpha)^{-1}$	α^2
D2	$-\ln(1-\alpha)$	$(1-\alpha)\ln(1-\alpha)+\alpha$
D3	$3/2(1-\alpha)^{2/3}[-1-(1-\alpha)]^{-1/3}$	$[1-(1-\alpha)^{1/3}]^2$
D4	$3/2(1-\alpha)^{1/3}[-1-(1-\alpha)]^{-1/3}$	$(1-2/3\alpha)(1-\alpha)^{2/3}$
F1	$(1-\alpha)$	$-\ln(1-\alpha)$
Power	$2\alpha^{1/2}$	$\alpha^{1/2}$
$n+m=2$; $n=1.5$	$\alpha^{0.5}(1-\alpha)^{1.5}$	$[(1-\alpha)\alpha]^{-0.5}(0.5)^{-1}$
$n=2$	$(1-\alpha)^2$	$-1+(1-\alpha)^{-1}$
$n=3$	$(1-\alpha)^3$	$2^{-1}[-1+(1-\alpha)^{-2}]$
$n=2.4$; $m=0.6$	$\alpha^{0.6}(1-\alpha)^{2.4}$	$[((1-\alpha)/\alpha)^{-1.4}/1.4]$ $+[((1-\alpha)/\alpha)^{-0.4}/0.4]$
$n+m=2$; $n=1.7$	$\alpha^{0.3}(1-\alpha)^{1.7}$	$[((1-\alpha)/\alpha)^{-0.7}/0.7]$
$n=1.5$	$(1-\alpha)^{1.5}$	$[1-(1-\alpha)^{-0.5}/0.5]$

An alternative to isothermal curing is the nonisothermal one made by DSC. One of the problems associated with this method is that the overall curing provides no kinetic information about the elemental processes.

In a previous study [16] using γ-BL, we determined that practically all the evolved heat in a dynamic experiment should be associated with the reactive processes in which epoxy groups participate, because the enthalpy per mol of epoxy group is about 95 kJ, whereas it is only 5 kJ by mol of lactone and 20 kJ per mol of SOE [16,38]. After complete curing all the epoxy and lactone groups have been opened and from the above mentioned enthalpies, the DGEBA/γ-VL 2:1 (mol/mol) formulation could evolve a theoretical enthalpy of 454, of which 448 J/g are associated to the opening of epoxides and 6 J/g to the lactone opening. Therefore, the kinetics obtained from nonisothermal experiments are expected to be similar to the kinetics obtained isothermally for the epoxy groups.

Fig. 9 shows the calorimetric curves of the nonisothermal curing of DGEBA with γ-VL at different heating rates. The shoulders that appear at low temperatures can be related with the contribution of the monomer activated mechanism (AM) that coexists with the activated chain mechanism (ACE) associated to the main peak, as

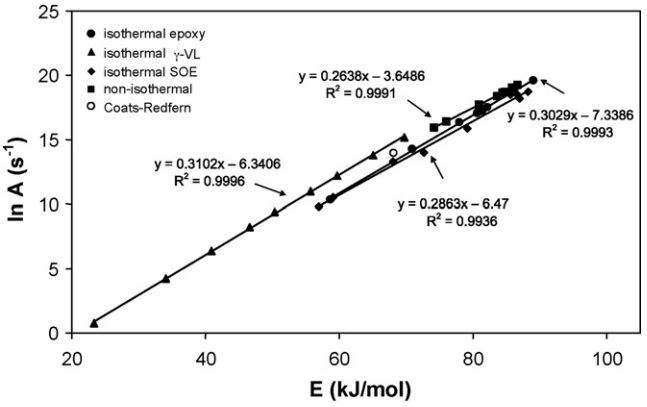

Fig. 8. Isokinetic relationships (IKRs) deduced from isothermal data associated with each reactive group and for nonisothermal data for the F1 model. The plot includes the point (○) corresponding to the Coats–Redfern adjustment for the F1 model.

Table 3
Isokinetic parameters obtained from the compensation curves for the different models used.

Model	Epoxy (910 cm^{-1})				γ-Valerolactone (1775 cm^{-1})				SOE (1737 cm^{-1})			
	a (mol/kJ)	b (s^{-1})	T_{iso} (°C)	r	a (mol/kJ)	b (s^{-1})	T_{iso} (°C)	r	a (mol/kJ)	b (s^{-1})	T_{iso} (°C)	r
A3/2	0.272	−4.686	170	0.9965	0.288	−5.094	144	0.9994	0.262	−4.476	186	0.9935
A2	0.256	−3.360	197	0.9933	0.277	−4.471	161	0.9995	0.250	−3.479	208	0.9919
A3	0.240	−2.033	228	0.9884	0.266	−3.847	178	0.9995	0.238	−2.482	232	0.9880
A4	0.232	−1.370	244	0.9851	0.261	−3.535	188	0.9995	0.232	−1.984	245	0.9866
R2	0.296	−7.980	134	0.9985	0.303	−7.237	124	0.9992	0.279	−7.161	158	0.9932
R3	0.292	−7.362	139	0.9980	0.300	−6.741	128	0.9989	0.276	−6.570	163	0.9927
D1	0.357	−12.803	64	0.9982	0.339	−9.040	82	0.9963	0.320	−10.288	103	0.9933
D2	0.368	−14.212	54	0.9983	0.349	−10.002	72	0.9974	0.331	−11.574	91	0.9913
D3	0.382	−16.580	42	0.9973	0.362	−11.873	59	0.9987	0.344	−13.833	76	0.9875
D4	0.373	−16.001	50	0.9981	0.353	−11.626	67	0.9979	0.335	−13.326	86	0.9902
F1	0.303	−7.339	124	0.9993	0.310	−6.341	115	0.9996	0.286	−6.470	147	0.9936
Power	0.246	−2.736	216	0.9881	0.268	−4.210	176	0.9990	0.240	−2.938	227	0.9909
$n+m=2$; $n=1.5$	0.269	−3.478	174	0.9970	0.290	−4.171	141	0.9995	0.263	−3.542	184	0.9897
$n=2$	0.329	−8.961	93	0.9975	0.336	−7.127	85	0.9995	0.313	−7.982	112	0.9820
$n=3$	0.360	−10.924	61	0.9881	0.368	−8.134	54	0.9960	0.345	−9.864	76	0.9596
$n=2.4$; $m=0.6$	0.278	−3.650	160	0.9963	0.304	−4.254	122	0.9979	0.277	−3.928	162	0.9775
$n+m=2$; $n=1.7$	0.293	−5.730	138	0.9988	0.309	−5.412	117	0.9994	0.283	−5.377	152	0.9879
$n=1.5$	0.315	−8.104	109	0.9992	0.322	−6.702	100	0.9995	0.299	−7.173	130	0.9892

T_{iso} (°C) calculated using $a = 1/RT_{iso}$.

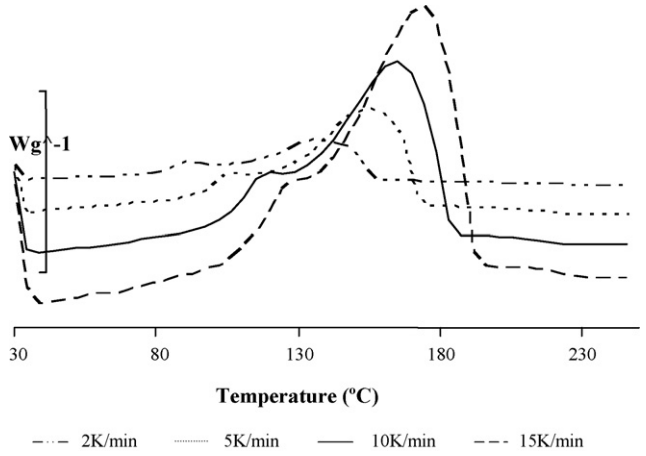

Fig. 9. DSC scanning curves vs. temperature for nonisothermal curing at different heating rates.

we described for similar DGEBA/γ-BL systems [13]. Fig. 10 shows the plot of conversion vs. curing temperature for the nonisothermal curing of DGEBA with γ-VL at different heating rates calculated by integration of the DSC curves (Fig. 9). Using Eq. (8) we determined

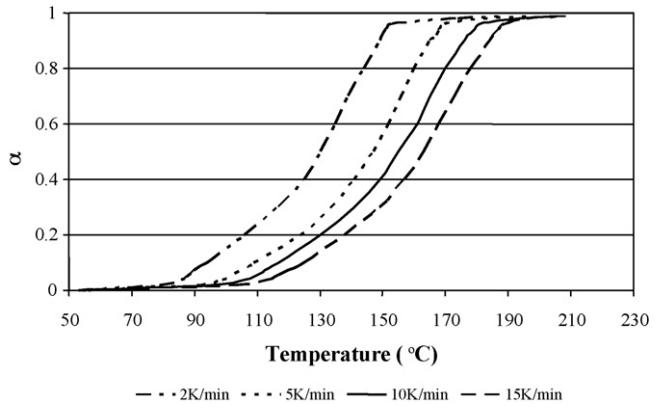

Fig. 10. Conversion degree vs. temperature, calculated according Eq. (2) for nonisothermal curing at different heating rates.

the isoconversional parameters and then we calculated the isothermal parameters from Eq. (4). From these parameters (Table 4) we simulated the conversion of epoxy groups, which are represented in Fig. 5. The goodness of the simulation (with the exception of a short deviation at low conversions, probably related with the contribution of AM mechanism in nonisothermal curing) and the regressions obtained (Table 4) in addition to the fact that the nonisothermal kinetic parameters are similar to those of epoxy groups, confirm that our assumptions are correct.

To determine the kinetic best-fit model from nonisothermal parameters we used two different strategies. Coats–Redfern method allows, by applying Eq. (7), to determine E and $\ln A$ for the different models. Table 5 shows all the results obtained at a heating rate of 15 K/min. We select F1 as the preferred model because it presents the best adjustment. Some other models also have good regressions, but we did no consider them because of E is quite different from that obtained isoconversionally (considered to be the true E). If the variation in the activation energy with the degree of conversion is taken into account, the kinetic model can be determined as in the isothermal case. From the nonisothermal values in Table 4, we calculated the IKRs for the different models. Table 5 shows the results. Again the F1 model gives the best regression and the T_{iso} of 183 °C practically lies in the experimental range of curing temperatures. In Table 4 we can see the pre-exponential factors determined from the isoconversional values by the F1 model and, in Fig. 8, we can see the different IKR for the different reactive groups and processes. The kinetic parameters determined by the Coats–Redfern

Table 4
Kinetic Parameters of nonisothermal Curing Obtained by DSC.

α	E (kJ/mol)	$\ln[AR/g(\alpha)E]$ (K/s)	$\ln[g(\alpha)/A]$ (s)	$\ln A$ (s^{-1})	r
0.1	74.2	0.15	−18.18	15.93	0.9960
0.2	76.0	0.15	−17.91	16.41	0.9845
0.3	80.9	0.16	−18.74	17.71	0.9906
0.4	84.4	0.17	−19.32	18.65	0.9950
0.5	83.7	0.16	−18.74	18.38	0.9936
0.6	84.9	0.16	−18.79	18.70	0.9953
0.7	84.7	0.15	−18.47	18.66	0.9959
0.8	86.6	0.16	−18.76	19.23	0.9985
0.9	85.8	0.15	−18.21	19.04	0.9994

The intercept and the slope of the isoconversional relationship $\ln[\beta/T^2] = \ln[AR/g(\alpha)E] - E/RT$ from the nonisothermal dates let us to obtain $\ln[AR/g(\alpha)E]$ and E. $\ln[g(\alpha)/A]$ was calculated on the basis of $\ln[AR/g(\alpha)E]$ and E. $\ln A$ was calculated using kinetic model F1 and $\ln[g(\alpha)/A]$.

Table 5
Arrhenius parameters determined by Coats–Redfern method and the isokinetics parameters [Eq. (9)].

Model	Coats–Redfern			Isokinetic relationship			
	E (kJ/mol)	$\ln A$ (s^{-1})	r	a (mol/kJ)	b (s^{-1})	T_{iso} (°C)	r
A3/2	6.7	14.88	0.9960	0.194	2.226	345	0.9909
A2	2.9	11.13	0.9599	0.160	5.164	479	0.9714
A3	−1.0	7.19	0.9947	0.125	8.101	688	0.9238
A4	−3.1	5.05	0.9933	0.108	9.570	843	0.8796
R2	57.5	9.96	0.9995	0.245	−3.298	219	0.9980
R3	60.8	10.60	0.9990	0.236	−2.228	237	0.9956
D1	104.1	23.20	0.9982	0.368	−13.507	54	0.9967
D2	122.1	28.82	0.9996	0.397	−16.366	30	0.9968
D3	128.8	28.56	0.9991	0.433	−20.572	5	0.9933
D4	119.7	25.77	0.9996	0.409	−18.760	21	0.9961
F1	68.1	13.97	0.9964	0.264	−3.649	183	0.9996
Power	20.7	−0.36	0.9968	0.134	7.105	626	0.9189
$n+m=2$; $n=1.5$	43.6	7.88	0.9765	0.195	3.209	344	0.9933
$n=2$	94.4	22.07	0.9796	0.334	−8.943	87	0.9792
$n=3$	126.5	31.84	0.9586	0.420	−15.446	13	0.9380
$n=2.4$; $m=0.6$	56.2	12.20	0.9308	0.228	1.078	254	0.9646
$n+m=2$; $n=1.7$	63.9	13.57	0.9784	0.251	−1.711	207	0.9917
$n=1.5$	80.4	17.79	0.9893	0.297	−6.124	132	0.9937

Isokinetic relationship obtained from Eq. (9).

method practically lays on the extrapolated nonisothermal IKR. This result confirms that the nonisothermal methodology used is correct to determinate the best-fit kinetic model.

5. Conclusions

FTIR spectroscopy allows analyzing the individual elemental chemical reactions that take part in a complex curing process, such as the cationic crosslinking of DGEBA/γ-VL mixtures. In this reactive system we determined the conversions and kinetics of the different epoxy, γ-VL and SOE reactive groups.

Calorimetric studies cannot separate the elemental processes and only provided the global kinetics of the crosslinking. If the elemental reactions have different enthalpies, the obtained results are only representative of the process with the highest enthalpy and extension.

Isoconversional methods make it possible the evaluation of the kinetic parameters on varying the degree of conversion, but they do not reveal the complete kinetic triplet. Using these methods, in combination with the isokinetic relationships in the isothermal and nonisothermal curing, it has been possible to calculate the complete kinetic triplet [E, A, $g(\alpha)$].

The kinetic parameters, in addition to the FTIR results, indicate that the reaction of γ-VL and epoxides is more favoured than the homopolymerization of epoxides or the ring-opening of SOE groups.

All the elemental reactions that participate in the curing of DGEBA epoxy resins with γ-VL catalyzed by ytterbium triflate followed an nth-order kinetic model, F1 type.

Acknowledgements

The authors from the Universitat Politècnica de Catalunya would like to thank CICYT and FEDER (MAT2004-04165-C02-02 and ENER2007-6784-C03-01) for their financial support. The authors from the Rovira i Virgili University would like to thank the CICYT (Comisión Interministerial de Ciencia y Tecnología) and FEDER (Fondo Europeo de Desarrollo Regional) (MAT2005-01806).

References

[1] S.G. Croll, J. Coat. Technol. 51 (1979) 49.
[2] R.K. Sadhir, M.R. Luck (Eds.), Expanding Monomers. Synthesis, Characterization and Applications, CRC Press, Boca Raton, FL, 1992.
[3] W.J. Bailey, R.L. Sun, Polym. Prep. Am. Chem. Soc., Div. Polym. Chem. 13 (1972) 400.
[4] W.J. Bailey, Elastoplast 5 (1973) 142.
[5] W.J. Bailey, J. Polym. Sci. Polym. Chem. Ed. 14 (1976) 1735.
[6] W.J. Bailey, R.L. Sun, H. Katsuki, T. Endo, H. Iwana, R. Tsushima, K. Saigou, M.M. Bitritto, Am. Chem. Soc. Symp. Ser. 59 (1977) 38.
[7] K. Bodenbenner, Justus Liebig Ann. 625 (1959) 183.
[8] M. Tokizava, N. Okada, N. Wakabayashi, J. Appl. Polym. Sci. 50 (1993) 875.
[9] K. Morio, H. Murase, H. Tsuchylla, T. Endo, J. Appl. Polym. Sci. 32 (1986) 5727.
[10] L. Matéjka, P. Chabanne, L. Tighzert, J.P. Pascault, J. Polym. Sci. Part A: Polym. Chem. 32 (1994) 1447.
[11] S. Kobayashi (Ed.), Lanthanides: Chemistry and Use in Organic Synthesis, Topics in Organometallic Chemistry, Springer Verlag, Berlin, 1999.
[12] S. Kobayashi, M. Sugiura, H. Kitagawa, W.W.L-. Lam, Chem. Rev. 102 (2002) 2227.
[13] C. Mas, A. Mantecón, A. Serra, X. Ramis, J.M. Salla, J. Polym. Sci. Part A: Polym. Chem. 42 (2004) 3782.
[14] L. González, X. Ramis, J.M. Salla, A. Mantecón, A. Serra, J. Polym. Sci. Part A: Polym. Chem. 44 (2006) 6869.
[15] M. Arasa, X. Ramis, J.M. Salla, A. Mantecón, A. Serra, J. Polym. Sci. Part A: Polym. Chem. 45 (2007) 2129.
[16] C. Mas, X. Ramis, J.M. Salla, A. Mantecón, A. Serra, J. Polym. Sci. Part A: Polym. Chem. 41 (2003) 2794.
[17] X. Ramis, A. Cadenato, J.M. Morancho, J.M. Salla, Polymer 44 (2003) 2067.
[18] S. Vyazovkin, W. Linert, Int. Rev. Phys. Chem. 14 (1995) 355.
[19] P. Budrugeac, D. Homentcovschi, E. Segal, J. Therm. Anal. Cal. 63 (2001) 457.
[20] J.M. Salla, X. Ramis, J.M. Morancho, A. Cadenato, Thermochim. Acta 388 (2002) 355.
[21] Z. Zhiqiang, J. Bangkun, H. Pingsheng, J. Appl. Polym. Sci. 84 (2002) 1457.
[22] H. Fridman, J. Polym. Chem. C6 (1963) 183.
[23] S. Vyazovkin, N. Sbirrazzuoli, Macromol. Chem. Phys. 200 (1999) 2294.
[24] A.W. Coats, J.P. Redfern, Nature 207 (1964) 290.
[25] S. Vyazovkin, D. Dollimore, J. Chem. Inform. Comput. Sci. 36 (1996) 42.
[26] H.E. Kissinger, Anal. Chem. 29 (1957) 1702.
[27] A. Cadenato, J.M. Morancho, X. Fernández-Francos, J.M. Salla, X. Ramis, Therm. Anal. Cal. 89 (2007) 233.
[28] J.H. Flynn, L.A. Wall, J. Res. Natl. Bur. Stad. A: Phys. Chem. 70A (1996) 487.
[29] T. Ozawa, Bull. Chem. Soc. Jpn. 38 (1965) 1881.
[30] X. Ramis, J.M. Salla, A. Cadenato, J.M. Morancho, Therm. Anal. Cal. 72 (2003) 707.
[31] X. Ramis, J.M. Salla, J. Polym. Sci. Part B: Polym. Phys. 35 (1997) 371.
[32] S. Vyazovkin, Int. J. Chem. Kinet. 28 (1996) 95.
[33] S. Vyazovkin, C.A. Wight, Annu. Rev. Phys. Chem. 48 (1997) 125.
[34] S. Vyazovkin, W. Linert, J. Solid State Chem. 114 (1995) 392.
[35] W. Linert, R.F. Jameson, Chem. Soc. Rev. 18 (1989) 477.
[36] S. Vyazovkin, W. Linert, Chem. Phys. 193 (1995) 109.
[37] X. Ramis, J.M. Salla, C. Mas, A. Mantecón, A. Serra, J. Appl. Polym. Sci. 92 (2004) 381.
[38] A.A. Yevstropov, B.V. Lebedev, Y.G. Kipararisova, V.A. Alekseyev, G.A. Stashina, Vysokomol. Soedin. Ser. A22 (1980) 2450.